

Precision Electroweak Physics at Future Collider Experiments¹

U. Baur²

Physics Department, SUNY Buffalo, Buffalo, NY 14260, USA

M. Demarteau²

Fermi National Accelerator Laboratory, P.O. Box 500, Batavia, IL 60510, USA

Working Group Members

C. Balazs (*MSU*), D. Errede (*Urbana*), S. Errede (*Urbana*), T. Han (*Davis*),
S. Keller (*FNAL*), Y-K. Kim (*Berkeley*), A.V. Kotwal (*Columbia*), F. Merritt (*Chicago*),
S. Rajagopalan (*Stony Brook*), R. Sobey (*Davis*), M. Swartz (*SLAC*),
D. Wackerlo (FNAL), J. Womersley (FNAL)

Abstract

We present an overview of the present status and prospects for progress in electroweak measurements at future collider experiments leading to precision tests of the Standard Model of Electroweak Interactions. Special attention is paid to the measurement of the W mass, the effective weak mixing angle, and the determination of the top quark mass. Their constraints on the Higgs boson mass are discussed.

¹To appear in the *Proceedings of the 1996 DPF/DPB Summer Study on New Directions for High-Energy Physics* (Snowmass 96), Snowmass, Colorado, June 25 – July 12, 1996

Work supported in part by the U.S. Dept. of Energy under contract DE-AC02-76CHO3000 and NSF grant PHY9600770

²Co-convener

Precision Electroweak Physics at Future Collider Experiments[‡]

U. Baur[§]

Physics Department, SUNY Buffalo, Buffalo, NY 14260

M. Demarteau[§]

Fermi National Accelerator Laboratory, P.O. Box 500, Batavia, IL 60510

Working Group Members

C. Balazs (*MSU*), D. Errede (*Urbana*), S. Errede (*Urbana*), T. Han (*Davis*), S. Keller (*FNAL*),
Y-K. Kim (*Berkeley*), A.V. Kotwal (*Columbia*), F. Merritt (*Chicago*), S. Rajagopalan (*Stony Brook*),
R. Sobey (*Davis*), M. Swartz (*SLAC*), D. Wackerlooh (*FNAL*), J. Womersley (*FNAL*)

ABSTRACT

We present an overview of the present status and prospects for progress in electroweak measurements at future collider experiments leading to precision tests of the Standard Model of Electroweak Interactions. Special attention is paid to the measurement of the W mass, the effective weak mixing angle, and the determination of the top quark mass. Their constraints on the Higgs boson mass are discussed.

I. INTRODUCTION

The Standard Model (SM) of strong and electroweak interactions, based on the gauge group $SU(3)_C \times SU(2)_L \times U(1)_Y$, has been extremely successful phenomenologically. It has provided the theoretical framework for the description of a very rich phenomenology spanning a wide range of energies, from the atomic scale up to the Z boson mass, M_Z . It is being tested at the level of a few tenths of a percent, both at very low energies and at high energies [1], and has correctly predicted the range of the top quark mass from loop corrections. However, the SM has a number of shortcomings. In particular, it does not explain the origin of mass, the observed hierarchical pattern of fermion masses, and why there are three generations of quarks and leptons. It is widely believed that at high energies, or in very high precision measurements, deviations from the SM will appear, signaling the presence of new physics.

In this report we discuss the prospects for precision tests of the Standard Model at future collider experiments, focussing on electroweak measurements. The goal of these measurements is to confront the SM predictions with experiment, and to derive indirect information on the mass of the Higgs boson. The existence of at least one Higgs boson is a direct consequence of spontaneous symmetry breaking, the mechanism which is

responsible for generating mass of the W and Z bosons, and fermions in the SM. In Section II we identify some of the relevant parameters for precision electroweak measurements, and review the present experimental situation. Expectations from future collider experiments are discussed in Section III. We conclude with a summary of our results.

II. CONSTRAINTS ON THE STANDARD MODEL FROM PRESENT ELECTROWEAK MEASUREMENTS

There are three fundamental parameters measured with high precision which play an important role as input variables in Electroweak Physics. The fine structure constant, $\alpha = 1/137.0359895$ is known with a precision of $\Delta\alpha = 0.045$ ppm. The muon decay constant, $G_\mu = 1.16639 \times 10^{-5}$ GeV $^{-2}$ is measured with $\Delta G_\mu = 17$ ppm from muon decay [2]. Finally, the Z boson mass, $M_Z = 91.1863$ GeV/c 2 [1] is measured with $\Delta M_Z = 22$ ppm in experiments at LEP and SLC. Knowing these three parameters, one can evaluate the W mass, M_W , and the weak mixing angle, $\sin^2 \theta_W$, at tree level. When loop corrections are taken into account, M_W and $\sin^2 \theta_W$ also depend on the top quark mass, M_t , and the Higgs boson mass, M_H . The two parameters depend quadratically on M_t , and logarithmically on M_H .

If the W mass and the top quark mass are precisely measured, information on the mass of the Higgs boson can be extracted. Constraints on the Higgs boson mass can also be obtained from the effective weak mixing angle and M_t . The ultimate test of the SM may lie in the comparison of these indirect determinations of M_H with its direct observation at future colliders.

The mass of the top quark is presently determined by the CDF and DØ collaborations from $t\bar{t}$ production at the Tevatron in the di-lepton, the lepton plus jets, and the all hadronic channels [3]. The combined value of the top quark mass from the lepton +

[‡] Work supported in part by the U.S. Dept. of Energy under contract DE-AC02-76CHO3000 and NSF grant PHY9600770

[§] Co-convenor

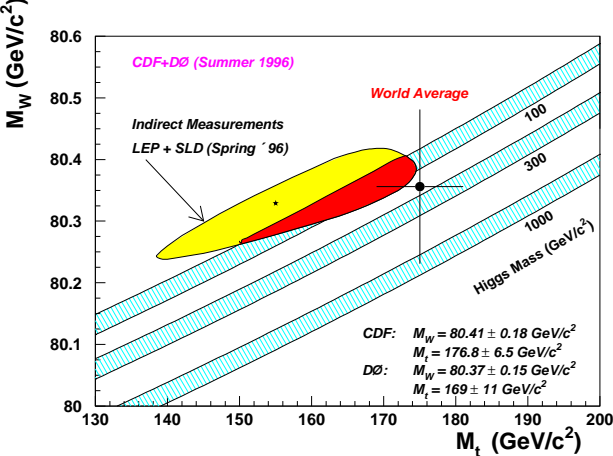


Figure 1: Comparison of the top quark and W boson masses from current direct and indirect measurements with the SM prediction.

jets channel, which yields the most precise result, is

$$M_t = 175 \pm 6 \text{ GeV}/c^2. \quad (1)$$

The W boson mass has been measured precisely by UA2, CDF, and DØ. Currently, the most accurate determination of M_W comes from the Tevatron CDF and DØ Run Ia analyses [4] and a preliminary DØ measurement [5] based on data taken during Run Ib. The current world average is [1]

$$M_W = 80.356 \pm 0.125 \text{ GeV}/c^2. \quad (2)$$

Figure 1 compares the results of the current M_W and M_t measurements in the (M_t, M_W) plane with those from indirect measurements at LEP and SLC [1], and the SM prediction for different Higgs boson masses. The cross hatched bands show the SM prediction for the indicated Higgs boson masses. The width of the bands is due primarily to the uncertainty on the electromagnetic coupling constant at the Z mass scale, $\alpha(M_Z^2)$, which has been taken to be $\alpha^{-1}(M_Z^2) = 128.89 \pm 0.10$. Recent estimates give $\delta\alpha(M_Z^2) \approx 0.0004 - 0.0007$ [6], which corresponds to $\delta\alpha^{-1}(M_Z^2) \approx 0.05 - 0.09$.

The uncertainty on $\alpha(M_Z^2)$ is dominated by the error on the hadronic contribution to the QED vacuum polarization which originates from the experimental error on the cross section for $e^+e^- \rightarrow \text{hadrons}$. Using dispersion relations [7], the hadronic contribution to $\alpha(M_Z^2)$ can be related to the cross section of the process $e^+e^- \rightarrow \text{hadrons}$ via

$$\Delta\alpha_{\text{had}}(M_Z^2) = \frac{\alpha M_Z^2}{3\pi} \mathcal{P} \int_{4m_\pi^2}^{\infty} \frac{R_{\text{had}}(s')}{s'(s' - M_Z^2)} ds', \quad (3)$$

where \mathcal{P} denotes the principal value of the integral, and

$$R_{\text{had}} = \frac{\sigma(e^+e^- \rightarrow \text{hadrons})}{\sigma(e^+e^- \rightarrow \mu^+\mu^-)}. \quad (4)$$

contributions at M_Z

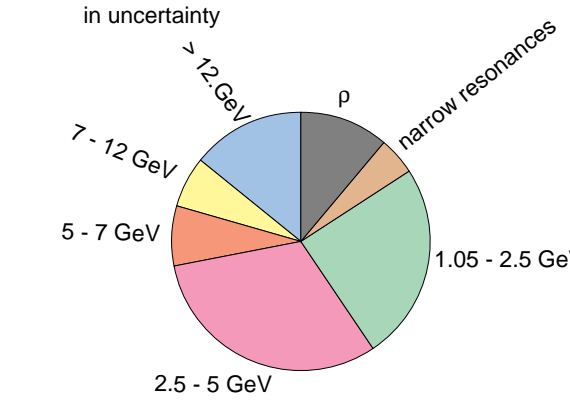
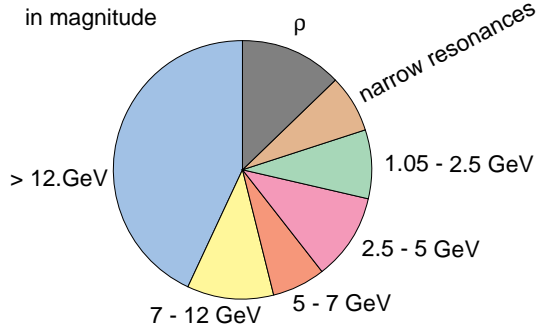


Figure 2: Relative contributions to $\Delta\alpha_{\text{had}}(M_Z^2)$ in magnitude and uncertainty.

The relative contributions to $\Delta\alpha_{\text{had}}(M_Z^2)$ and the uncertainty are detailed in Fig. 2 [6]. About 60% of the uncertainty comes from the energy region between 1.05 GeV and 5 GeV. More precise measurements of the total hadronic cross section in this energy region, for example at Novosibirsk, DAPFNE or BES may reduce the uncertainty on $\alpha(M_Z^2)$ by about a factor 2 in the near future.

The W mass can also be determined indirectly from radiative corrections to electroweak observables at LEP and SLD, and from νN scattering experiments. The current indirect value of M_W obtained from e^+e^- experiments, $M_W = 80.337 \pm 0.041^{+0.010}_{-0.021} \text{ GeV}/c^2$ [1], is in excellent agreement with the result obtained from direct measurements (see Fig. 1). The determination of M_W from νN scattering will be discussed in Section III.C.

The effective weak mixing angle, $\sin^2 \theta_{eff}^{lept}$, has been determined with high precision from measurements of the forward backward asymmetries at LEP, and the left-right asymmetries

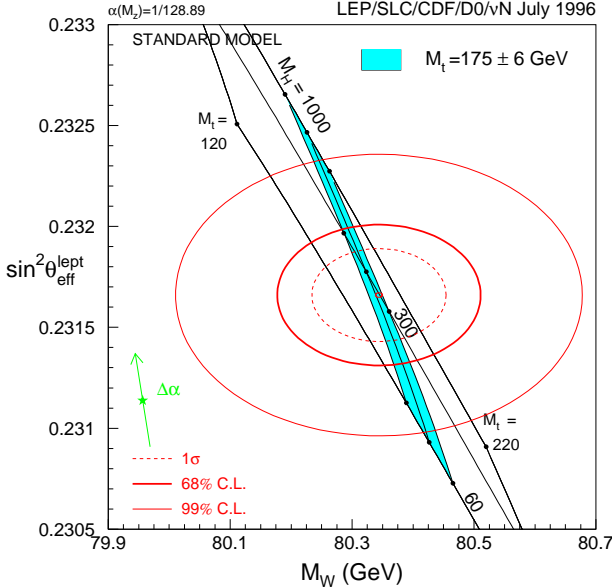


Figure 3: Comparison of $\sin^2 \theta_{\text{eff}}^{\text{lept}}$ and the W boson mass from current direct and indirect measurements with the SM prediction. The top quark and Higgs boson masses indicated in the figure are all in GeV/c^2 .

at the SLC [1]. Here, $\sin^2 \theta_{\text{eff}}^{\text{lept}}$ is defined by

$$\sin^2 \theta_{\text{eff}}^{\text{lept}} = \frac{1}{4} \left(1 - \frac{g_{V\ell}}{g_{A\ell}} \right), \quad (5)$$

where $g_{V\ell}$ and $g_{A\ell}$ are the effective vector and axial vector coupling constants of the leptons to the Z boson, and is related to the weak mixing angle in the $\overline{\text{MS}}$ scheme, $\sin^2 \hat{\theta}_W(M_Z)$, by [8]

$$\sin^2 \theta_{\text{eff}}^{\text{lept}} \approx \sin^2 \hat{\theta}_W(M_Z) + 0.00028. \quad (6)$$

A fit to the combined LEP and SLD asymmetry data yields

$$\sin^2 \theta_{\text{eff}}^{\text{lept}} = 0.23165 \pm 0.00024. \quad (7)$$

The experimental constraints in the $(\sin^2 \theta_{\text{eff}}^{\text{lept}}, M_W)$ plane are compared with the SM predictions in Fig. 3. The measured value of $\sin^2 \theta_{\text{eff}}^{\text{lept}}$ agrees well with the SM expectation. The star in the lower lefthand corner of Fig. 3 indicates the W mass and effective weak mixing angle predicted by taking the running of α into account only. The arrow represents the current uncertainty on M_W and the effective weak mixing angle from $\Delta \alpha_{\text{had}}(M_Z^2)$:

$$\delta \sin^2 \theta_{\text{eff}}^{\text{lept}}|_{\Delta \alpha} = 0.00023, \quad (8)$$

$$\delta M_W|_{\Delta \alpha} = 12 \text{ MeV}/c^2. \quad (9)$$

The estimated theoretical error from higher orders introduces an additional uncertainty of [9]

$$\delta \sin^2 \theta_{\text{eff}}^{\text{lept}}|_{\text{th}} = 0.00008, \quad (10)$$

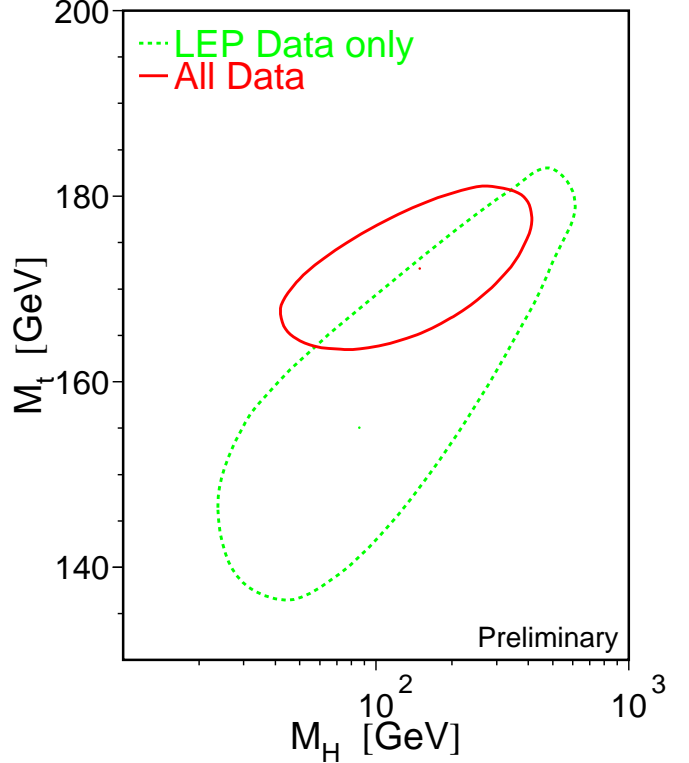


Figure 4: The 68% confidence level contours in M_t and M_H for the fits to LEP data only (dashed curve) and to all data (solid curve).

$$\delta M_W|_{\text{th}} = 9 \text{ MeV}/c^2. \quad (11)$$

While direct measurements of M_t and M_W presently do not impose any constraints on the Higgs boson mass, indirect measurements from LEP and SLD seem to indicate a preference for a relatively light Higgs boson. The 68% confidence level contours in the M_t and M_H plane for the fits to LEP data only, and to all data sets [1] (LEP, SLD, CDF and D \emptyset), are shown in Fig. 4. Taking the theoretical error due to missing higher order corrections into account, one obtains

$$M_H = 149_{-82}^{+148} \text{ GeV}/c^2, \quad (12)$$

or

$$M_H < 550 \text{ GeV}/c^2 \quad \text{at} \quad 95\% \text{ CL}. \quad (13)$$

The results of such a fit from current data, however, should be interpreted with caution. Removing one or two quantities from the fit can drastically change the predicted Higgs boson mass range. Excluding from the fit the hadronic width of the Z boson, which depends on α_s , results in [10]

$$M_H = (560 \times 1.5^{\pm 1}) \text{ GeV}/c^2. \quad (14)$$

Omitting in addition the SLD data on A_{LR} which yield a somewhat low value for the effective weak mixing angle, leads to $M_H = (820 \times 1.7^{\pm 1}) \text{ GeV}/c^2$.

In the future, only marginal improvements of the indirect measurements from LEP data are expected since LEP data taking at the Z peak has ceased. However, a significant reduction of the errors on M_t and M_W from direct experiments at LEP2, the Tevatron (Run I, Run II and TeV33), the LHC, and perhaps the NLC and/or a $\mu^+\mu^-$ collider is expected, which should result in a more stable prediction for M_H . This will be discussed in more detail in the next Section.

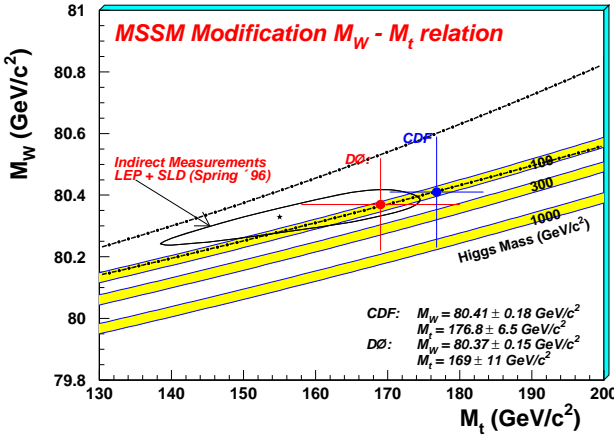


Figure 5: Predictions for M_W as a function of M_t in the SM (shaded bands) and in the MSSM (area between the dot-dashed lines). The results from direct CDF and DØ measurements, and from indirect measurements at LEP and SLD are also shown.

Precise measurements of M_W and M_t , if inconsistent with the range allowed by the SM, could indicate the existence of new phenomena at or above the electroweak scale, such as supersymmetry. In the near future direct and indirect measurements of the top quark and W boson mass are expected to begin to yield useful constraints on the parameter space of the minimal supersymmetric standard model (MSSM). This is illustrated in Fig. 5, where the predictions for M_W as a function of M_t in the SM (shaded bands) and in the MSSM (area between the dashed lines) are shown, together with results from direct CDF and DØ measurements, and indirect measurements from LEP and SLD. The MSSM band has been obtained by varying the model parameters so that they are consistent with current experimental data. In addition, it was assumed that no supersymmetric particles are found at LEP2 [11].

III. HIGH PRECISION ELECTROWEAK PHYSICS AT FUTURE COLLIDERS

A. Measurement of the Top Quark Mass

The prospects of measuring the top quark mass in future collider experiments are discussed in detail in Ref. [12]. We therefore only briefly summarize the results here.

For the Tevatron, the expected accuracy in M_t for Run II ($\int \mathcal{L} dt = 2 \text{ fb}^{-1}$) and for TeV33 ($\int \mathcal{L} dt = 10 - 30 \text{ fb}^{-1}$) can be extrapolated using current and anticipated CDF and DØ acceptances and efficiencies, together with theoretical predictions. Using various different methods and techniques [13], one expects that M_t can be determined to $\leq 4 \text{ GeV}/c^2$ ($\leq 2 \text{ GeV}/c^2$) in Run II (TeV33). The uncertainty on the top quark mass will be dominated by systematic errors. Soft and hard gluon radiation, and the jet transverse energy scale constitute the most important sources of systematic errors in the top quark mass measurement at hadron colliders. At the LHC, one also expects a precision of about $2 \text{ GeV}/c^2$ for M_t [12].

At an e^+e^- Linear Collider (NLC) or a $\mu^+\mu^-$ collider, the top quark mass can be determined with very high precision from a threshold scan. For an integrated luminosity of 10 fb^{-1} (50 fb^{-1}), the expected uncertainty on M_t at the NLC is $\delta M_t \approx 500 \text{ MeV}/c^2$ ($200 \text{ MeV}/c^2$) [14]. At a $\mu^+\mu^-$ collider, the reduced beamstrahlung and initial state radiation result in a better beam energy resolution which should make it possible to measure the top quark mass with a somewhat higher precision than at the NLC, for equal integrated luminosities. Simulations suggest $\delta M_t \approx 300 \text{ MeV}/c^2$ for 10 fb^{-1} [15].

The precision which can be achieved for M_t at different colliders is summarized in Table I. In our subsequent calculations

Table I: Expected top quark mass precision at future colliders.

Collider	δM_t
Tevatron (2 fb^{-1})	$4 \text{ GeV}/c^2$
TeV33 (10 fb^{-1})	$2 \text{ GeV}/c^2$
LHC (10 fb^{-1})	$2 \text{ GeV}/c^2$
NLC (10 fb^{-1})	$0.5 \text{ GeV}/c^2$
$\mu^+\mu^-$ (10 fb^{-1})	$0.3 \text{ GeV}/c^2$

we shall always assume that the top quark mass can be determined with a precision of

$$\delta M_t = 2 \text{ GeV}/c^2. \quad (15)$$

B. Measurement of $\sin^2 \theta_{eff}^{lept}$

1. SLD

Presently, the single most precise determination of the effective weak mixing angle originates from the measurement of the left-right asymmetry,

$$A_{LR} = \frac{\sigma_L - \sigma_R}{\sigma_{tot}} \quad (16)$$

at SLD. Here, $\sigma_{L(R)}$ is the total production cross section for left-handed (righthanded) electrons. In the SM, the left-right asymmetry at the Z pole, ignoring photon exchange contributions, is related to the effective weak mixing angle by

$$A_{LR} = \frac{2(1 - 4 \sin^2 \theta_{eff}^{lept})}{1 + (1 - 4 \sin^2 \theta_{eff}^{lept})^2}. \quad (17)$$

If the planned luminosity upgrade [16] (“SLC2000”) can be realized, it will be possible to collect 3×10^6 Z decays over a period of three to four years at SLD. This should result in an uncertainty of

$$\delta \sin^2 \theta_{eff}^{lept} = 0.00012, \quad (18)$$

which is approximately a factor 2 better than the current uncertainty from the fit to the combined LEP and SLD asymmetry data (see Eq. (7)).

Further improvements could come from measurements of the left-right forward-backward asymmetry in $e^+e^- \rightarrow \bar{f}f$,

$$\begin{aligned} \tilde{A}_{FB}^f(z) &= \frac{[\sigma_L^f(z) - \sigma_L^f(-z)] - [\sigma_R^f(z) - \sigma_R^f(-z)]}{[\sigma_L^f(z) + \sigma_L^f(-z)] + [\sigma_R^f(z) + \sigma_R^f(-z)]} \\ &= \frac{2g_{Vf}g_{Af}}{g_{Vf}^2 + g_{Af}^2} \frac{2z}{1+z^2}, \end{aligned} \quad (19)$$

where $z = \cos \theta$, and θ is the scattering angle. \tilde{A}_{FB}^f directly measures the coupling of the final state fermion f to the Z boson from which it is straightforward to determine $\sin^2 \theta_{eff}^{lept}$. In particular, with the self-calibrating jet-charge technique [17], a precise measurement of the $Z\bar{b}b$ coupling should be possible.

2. Hadron Colliders

At hadron colliders, the forward backward asymmetry, A_{FB} , in di-lepton production, $p\bar{p} \xrightarrow{(\rightarrow)} \ell^+\ell^-X$, ($\ell = e, \mu$), makes it possible to measure the effective weak mixing angle. A_{FB} is defined by

$$A_{FB} = \frac{F - B}{F + B}, \quad (20)$$

where

$$F = \int_0^1 \frac{d\sigma}{d\cos \theta^*} d\cos \theta^*, \quad (21)$$

$$B = \int_{-1}^0 \frac{d\sigma}{d\cos \theta^*} d\cos \theta^*, \quad (22)$$

and $\cos \theta^*$ is the angle between the lepton and the incoming quark in the $\ell^+\ell^-$ rest frame. In $p\bar{p}$ collisions at Tevatron energies, the flight direction of the incoming quark to a good approximation coincides with the proton beam direction. $\cos \theta^*$ can then be related to the components of the lepton and anti-lepton four-momenta via [18]

$$\cos \theta^* = 2 \frac{p^+(\ell^-)p^-(\ell^+) - p^-(\ell^-)p^+(\ell^+)}{m(\ell^+\ell^-)\sqrt{m^2(\ell^+\ell^-) + p_T^2(\ell^+\ell^-)}} \quad (23)$$

with

$$p^\pm = \frac{1}{\sqrt{2}}(E \pm p_z). \quad (24)$$

Here, $m(\ell^+\ell^-)$ is the invariant mass of the lepton pair, E is the energy, and p_z is the longitudinal component of the momentum vector. In this definition of $\cos \theta^*$, the polar axis is defined to be the bisector of the proton beam momentum and the negative of the anti-proton beam momentum when they are boosted into the $\ell^+\ell^-$ rest frame. The four-momenta of the quark and anti-quark cannot be determined individually. The definition of

$\cos \theta^*$ in Eq. (23) has the advantage of minimizing the effects of the momentum ambiguity induced by the parton transverse momentum.

First measurements of the effective weak mixing angle using the forward backward asymmetry at hadron colliders have been performed by the UA1 and CDF collaborations [19, 20]. Figure 6a shows the variation of A_{FB} with the e^+e^- invariant mass in $p\bar{p} \rightarrow e^+e^-$ for $\sqrt{s} = 1.8$ TeV, assuming $\sin^2 \theta_{eff}^{lept} = 0.232$. The error bars indicate the statistical errors for 100,000 events, corresponding to an integrated luminosity of about 2 fb^{-1} . The largest asymmetries occur at di-lepton invariant masses of

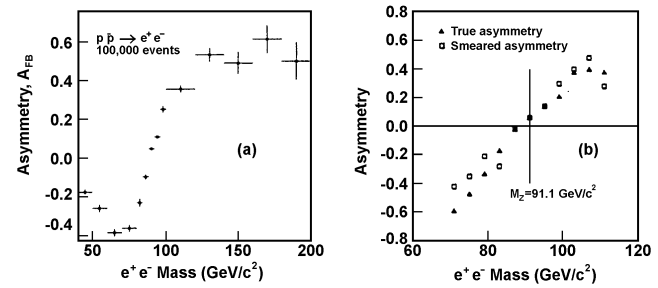


Figure 6: The forward backward asymmetry, A_{FB} , as a function of the e^+e^- invariant mass in $p\bar{p} \rightarrow e^+e^-$ events. (a) statistical error for 100,000 events, corresponding to an integrated luminosity of 2 fb^{-1} in an ideal detector; (b) including the effects of the D0 di-electron mass resolution.

around 70 GeV/c^2 and above 110 GeV/c^2 . A preliminary study of the systematic errors, indicates that most sources of error are small compared with the statistical error. The main contribution to the systematic error originates from the uncertainty in the parton distribution functions. Since the vector and axial vector couplings of u and d quarks to the Z boson are different, the measured asymmetry depends on the ratio of u to d quarks in the proton. Most of the systematic errors are expected to scale with $1/\sqrt{N}$, where N is the number of events. The effect of the electromagnetic calorimeter resolution is rather moderate, as shown in Fig. 6b. It is found that most of the sensitivity of this measurement to $\sin^2 \theta_{eff}^{lept}$ is at $m(e^+e^-) \approx M_Z$ due to the strong variation of A_{FB} with $\sin^2 \theta_{eff}^{lept}$ and the high statistics in this region. Including QED radiative corrections, the $p\bar{p} \rightarrow e^+e^-$ forward backward asymmetry in the Z boson resonance region ($75 \text{ GeV}/c^2 < m(e^+e^-) < 105 \text{ GeV}/c^2$) can be parameterized in terms of the effective weak mixing angle by [21]

$$A_{FB} = 3.6 (0.2464 - \sin^2 \theta_{eff}^{lept}). \quad (25)$$

The expected precision of $\sin^2 \theta_{eff}^{lept}$ in the electron channel (per experiment) versus the integrated luminosity at the Tevatron is shown in Fig. 7, together with the combined current uncertainty from LEP and SLD experiments. A similar precision is expected in the muon channel. Combining the results of the

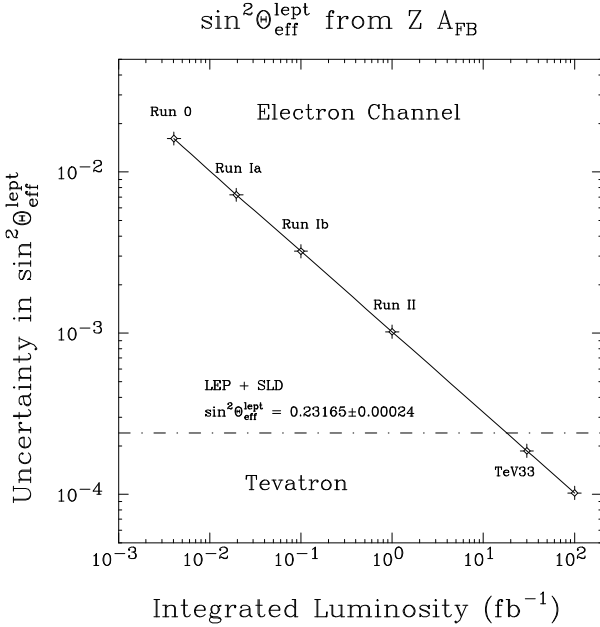


Figure 7: Projected uncertainty (per experiment) in $\sin^2 \theta_{\text{eff}}^{\text{lept}}$ from the measurement of A_{FB} in the Z pole region at the Tevatron versus the integrated luminosity.

electron and the muon channel, an overall uncertainty per experiment of

$$\delta \sin^2 \theta_{\text{eff}}^{\text{lept}} = 0.00013 \quad (26)$$

is expected for an integrated luminosity of 30 fb^{-1} .

At the LHC, the lowest order $Z \rightarrow \ell^+ \ell^-$ cross section is approximately 1.6 nb for each lepton flavor. For the projected yearly integrated luminosity of 100 fb^{-1} , this results in a very large number of $Z \rightarrow \ell^+ \ell^-$ events which, in principle, could be utilized to measure the forward backward asymmetry and thus $\sin^2 \theta_{\text{eff}}^{\text{lept}}$ with extremely high precision [22]. Since the original quark direction is unknown in pp collisions, one has to extract the angle between the lepton and the quark in the $\ell^+ \ell^-$ rest frame from the boost direction of the di-lepton system with respect to the beam axis:

$$\cos \theta^* = 2 \frac{|p_z(\ell^+ \ell^-)|}{p_z(\ell^+ \ell^-)} \frac{p^+(\ell^-)p^-(\ell^+) - p^-(\ell^-)p^+(\ell^+)}{m(\ell^+ \ell^-) \sqrt{m^2(\ell^+ \ell^-) + p_T^2(\ell^+ \ell^-)}}. \quad (27)$$

in order to arrive at a non-zero forward-backward asymmetry.

In contrast to Tevatron energies, sea quark effects dominate at the LHC. As a result, the probability, f_q , that the quark direction and the boost direction of the di-lepton system coincide is significantly smaller than one. This considerably reduces the forward backward asymmetry. Events with a large rapidity of the di-lepton system, $y(\ell^+ \ell^-)$, originate from collisions where at least one of the partons carries a large fraction x of the proton momentum. Since valence quarks dominate at high values of x , a cut on the di-lepton rapidity increases f_q , and thus the

asymmetry [23] and the sensitivity to the effective weak mixing angle.

Imposing a $|y(\mu^+ \mu^-)| > 1$ cut and including QED corrections, the forward backward asymmetry at the LHC in the $\mu^+ \mu^-$ channel in the Z peak region ($75 \text{ GeV}/c^2 < m(\mu^+ \mu^-) < 105 \text{ GeV}/c^2$) can be parameterized by

$$A_{FB} = 2.10 (0.2466 - \sin^2 \theta_{\text{eff}}^{\text{lept}}) \quad (28)$$

for an ideal detector. For an integrated luminosity of 100 fb^{-1} , this then leads to an expected error of

$$\delta \sin^2 \theta_{\text{eff}}^{\text{lept}} = 4.5 \times 10^{-5}. \quad (29)$$

A similar precision should be achievable in the electron channel.

However, electrons and muons can only be detected for pseudorapidities $|\eta(\ell)| < 2.4 - 3.0$ in the currently planned configurations of the ATLAS [24] and CMS [25] experiments at the LHC. The finite pseudorapidity range available dramatically reduces the asymmetry. In the region around the Z pole, the asymmetry is again approximately a linear function of $\sin^2 \theta_{\text{eff}}^{\text{lept}}$ with (for $\mu^+ \mu^-$ final states)

$$A_{FB} = 0.65 (0.2488 - \sin^2 \theta_{\text{eff}}^{\text{lept}}) \text{ for } |\eta(\mu)| < 2.4. \quad (30)$$

The finite rapidity coverage also results in a reduction of the total Z boson cross section by roughly a factor 5. As a result, the uncertainty expected for $\sin^2 \theta_{\text{eff}}^{\text{lept}}$ increases by almost a factor 7 to

$$\delta \sin^2 \theta_{\text{eff}}^{\text{lept}} = 3.0 \times 10^{-4} \text{ for } |\eta(\mu)| < 2.4. \quad (31)$$

In order to improve the precision beyond that expected from future SLC and Tevatron experiments, it will be necessary to detect electrons and muons in the very forward pseudorapidity range, $|\eta| = 3.0 - 5.0$, at the LHC.

3. NLC and $\mu^+ \mu^-$ Collider

The effective weak mixing angle can also be measured at the NLC in fixed target Møller and Bhabha scattering. In fixed target Møller scattering one hopes to achieve a precision of $\delta \sin^2 \theta_{\text{eff}}^{\text{lept}} = 6 \times 10^{-5}$ [26]. In Bhabha scattering, it should be possible to measure the effective weak mixing angle with a precision of a few $\times 10^{-4}$ [27], depending on the energy and polarization available. Possibilities to determine the effective weak mixing angle at a $\mu^+ \mu^-$ collider have not been investigated so far.

4. Constraints on M_H from $\sin^2 \theta_{\text{eff}}^{\text{lept}}$ and M_t

The potential of extracting useful information on the Higgs boson mass from a fit to the SM radiative corrections and a precise measurement of $\sin^2 \theta_{\text{eff}}^{\text{lept}}$ and M_t is illustrated in Fig. 8. Here we have assumed $M_t = 176 \pm 2 \text{ GeV}/c^2$, $\sin^2 \theta_{\text{eff}}^{\text{lept}} = 0.23143 \pm 0.00015$, and $\alpha^{-1}(M_Z^2) = 128.89 \pm 0.05$. From such a measurement, one would find $M_H = 415^{+145}_{-105} \text{ GeV}/c^2$. The corresponding log-likelihood function is shown in Fig. 9. From Fig. 8 it is obvious that the extracted Higgs boson mass

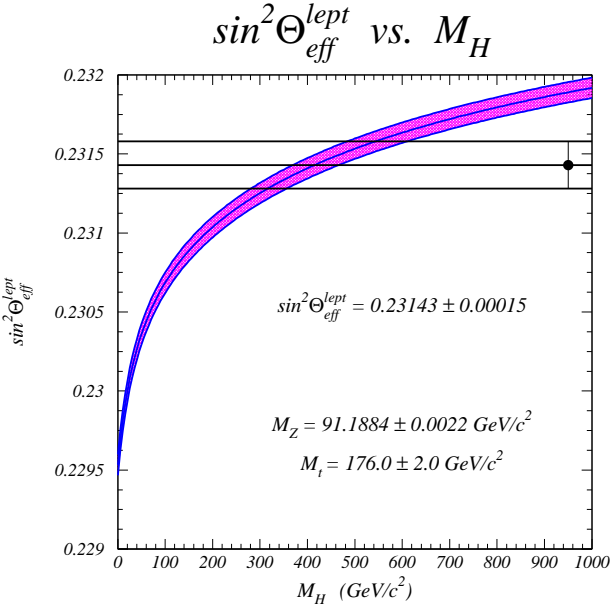


Figure 8: Predicted $\sin^2 \theta_{\text{eff}}^{\text{lept}}$ versus the Higgs boson mass.

depends very sensitively on the central value of the effective weak mixing angle. The relative error on the Higgs boson mass, $\delta M_H/M_H \approx 30\%$, however, depends only on the uncertainty of higher order corrections, $\sin^2 \theta_{\text{eff}}^{\text{lept}}$, M_t , and $\alpha(M_Z^2)$. For the precision of $\sin^2 \theta_{\text{eff}}^{\text{lept}}$ and M_t assumed here, the theoretical error from higher orders, and the uncertainty in $\alpha(M_Z^2)$ begin to limit the accuracy which can be achieved for the Higgs boson mass.

C. Precision Measurement of M_W at Future Experiments

1. Deep Inelastic Scattering and HERA

Future experiments provide a variety of opportunities to measure the mass of the W boson with high precision. In νN scattering, M_W can be determined indirectly through a measurement of the neutral to charged current cross section ratio

$$R_\nu = \frac{\sigma(\nu N \rightarrow \nu X)}{\sigma(\nu N \rightarrow \mu^- X)}. \quad (32)$$

In the SM, R_ν can be used to directly determine the weak mixing angle via the lowest order expression

$$R_\nu = \frac{1}{2} - \sin^2 \theta_W + \frac{5}{9} (1+r) \sin^4 \theta_W + C_\nu, \quad (33)$$

where

$$r = \frac{\sigma(\bar{\nu} N \rightarrow \mu^+ X)}{\sigma(\nu N \rightarrow \mu^- X)}, \quad (34)$$

and C_ν is a correction factor which incorporates, among others, effects due to charm production and longitudinal structure

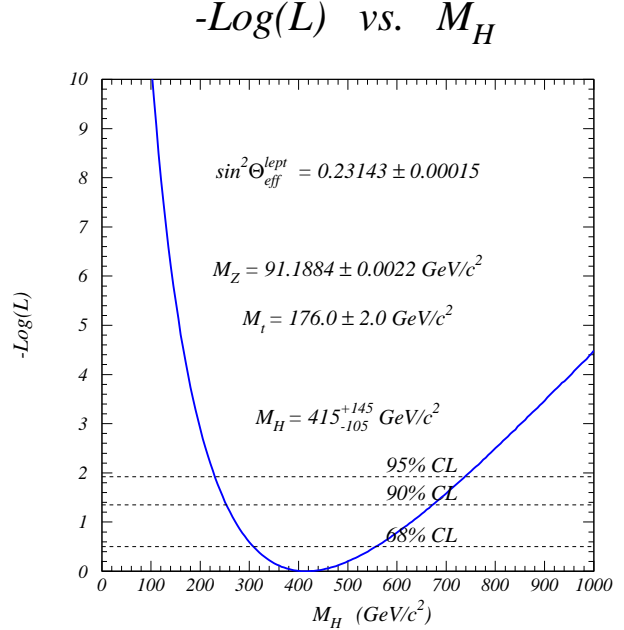


Figure 9: The negative log-likelihood function assuming $\sin^2 \theta_{\text{eff}}^{\text{lept}} = 0.23143 \pm 0.00015$ and $M_t = 176 \pm 2 \text{ GeV}/c^2$.

functions. Electroweak radiative corrections modify the leading order prediction. In the on-shell scheme, where $\sin^2 \theta_W = 1 - M_W^2/M_Z^2$ to all orders in perturbation theory, the (leading) radiative corrections to $\sin^2 \theta_W$ and R_ν almost perfectly cancel [28]. This implies that, in the SM, νN scattering directly measures the W mass, given the very precisely determined Z boson mass. A new CCFR measurement [29] gives $M_W = 80.46 \pm 0.25 \text{ GeV}/c^2$. With the data which one hopes to collect in the NuTeV experiment during the current Fermilab fixed target run, one expects [29]

$$\delta M_W \approx 100 \text{ MeV}/c^2. \quad (35)$$

Figure 10 compares the current results for M_W from direct measurements at CDF, DØ and LEP2 (see below) with indirect determinations from LEP and SLD via electroweak radiative corrections, and the W mass obtained from CCFR, other νN experiments [30], and the expectation for NuTeV.

The W mass can also be determined from measurements of the charged and neutral current cross sections at HERA. Moving the low β quadrupoles closer to the interaction region, one hopes to achieve integrated luminosities of the order of 150 pb^{-1} per year with a 70% longitudinally polarized electron beam. The expected constraints on M_W and M_t , together with the SM predictions for $M_H = 100 \text{ GeV}/c^2$ and $M_H = 800 \text{ GeV}/c^2$ are shown in Fig. 11 [31]. When combined with a measurement of the top quark mass with a precision of $\delta M_t = 5 \text{ GeV}/c^2$, the projected HERA results yield a precision

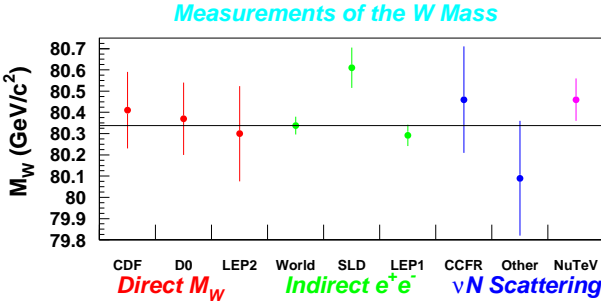


Figure 10: A comparison of direct and indirect measurements of the W boson mass.

of

$$\delta M_W \approx 60 \text{ MeV}/c^2. \quad (36)$$

Taking $\delta M_t = 2 \text{ GeV}/c^2$ instead only marginally improves the accuracy on the W mass. In deriving the result shown in Eq. (36), a 1% relative systematic uncertainty of the charged and neutral current cross sections at HERA was assumed. For a systematic error of 2%, one finds $\delta M_W \approx 80 \text{ MeV}/c^2$.

2. LEP2 and NLC

Precise measurements of the W mass at LEP2 [32] can be obtained using the enhanced statistical power of the rapidly varying total W^+W^- cross section at threshold [33], and the sharp (Breit-Wigner) peaking behaviour of the invariant mass distribution of the W decay products. During the recent LEP2 run at $\sqrt{s} = 161 \text{ GeV}$, the four LEP experiments have each accumulated approximately 10 pb^{-1} of data. The total W^+W^- cross section as a function of the W mass is shown in Fig. 12, together with the preliminary experimental result [34]. Combining the results obtained from the $W^+W^- \rightarrow jjjj$, the $W^+W^- \rightarrow \ell^\pm \nu jj$ and the $W^+W^- \rightarrow \ell^+ \nu \ell^- \nu$ ($\ell = e, \mu, \tau$) channel, the W pair production cross section at $\sqrt{s} = 161 \text{ GeV}$ is measured to be $\sigma(WW) = 3.57 \pm 0.46 \text{ pb}$. This translates into a W mass of [34]

$$M_W = 80.4 \pm 0.2 \pm 0.1 \text{ GeV}/c^2. \quad (37)$$

A much more accurate measurement of M_W will be possible in the future through direct reconstruction methods when LEP2 will be running at energies well above the W pair threshold. Here, the Breit-Wigner resonance shape is directly reconstructed from the W^\pm final states using kinematic fitting techniques. The potentially most important limitation in using this method originates from color reconnection [35] and Bose-Einstein correlations [36] in the $W^+W^- \rightarrow jjjj$ channel. Taking common errors into account, the expected overall precision from this method at LEP2 for a total integrated luminosity of 500 pb^{-1} per experiment is anticipated to be [32]

$$\delta M_W = 35 - 45 \text{ MeV}/c^2. \quad (38)$$

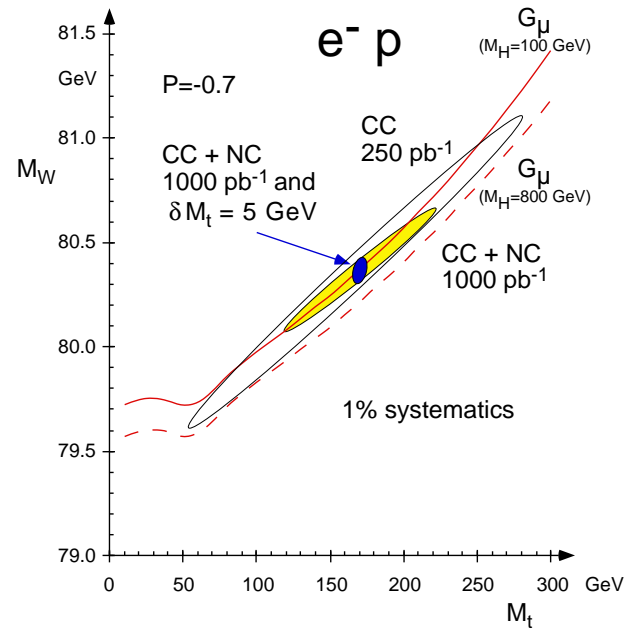


Figure 11: 1σ confidence contours in the (M_W, M_t) plane from polarized electron scattering at HERA ($P = -0.7$), utilizing charged current scattering alone for $\int \mathcal{L} dt = 250 \text{ pb}^{-1}$ (outer ellipse), and neutral and charged current scattering for 1 fb^{-1} (shaded ellipse). Shown is also the combination of the 1 fb^{-1} result with a direct top mass measurement with $\delta M_t = 5 \text{ GeV}/c^2$ (full ellipse). The SM predictions are also shown for two values of M_H (from Ref. [31]).

The same method can in principle also be used at the NLC. However, the beam energy spread limits the precision which one can hope to achieve at an e^+e^- Linear Collider. Preliminary studies indicate that one can hope for a precision of $\delta M_W = 20 \text{ MeV}/c^2$ at best. No studies for a $\mu^+\mu^-$ collider have been performed so far.

3. Tevatron

In W events produced in a hadron collider in essence only two quantities are measured: the lepton momentum and the transverse momentum of the recoil system. The latter consists of the “hard” W -recoil and the underlying event contribution. For W -events these two are inseparable. The transverse momentum of the neutrino is then inferred from these two observables. Since the longitudinal momentum of the neutrino cannot be determined unambiguously, the W -boson mass is usually extracted from the distribution in transverse:

$$M_T = \sqrt{2 p_T(e) p_T(\nu) (1 - \cos \varphi^{e\nu})}, \quad (39)$$

where $\varphi^{e\nu}$ is the angle between the electron and neutrino in the transverse plane. The M_T distribution sharply peaks at $M_T \approx$

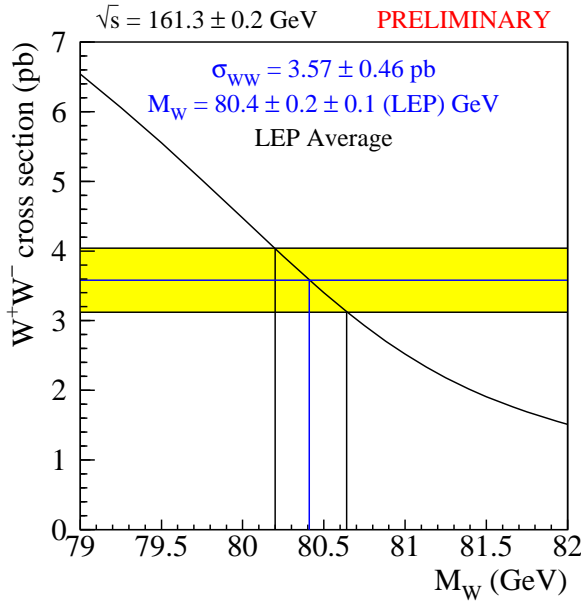


Figure 12: The total W^+W^- cross section as a function of the W boson mass. The shaded band represents the cross section measured at LEP2.

M_W .

Both the transverse mass and lepton transverse momentum are, by definition, invariant under longitudinal Lorentz boosts. In determining the W mass, the transverse mass is preferred over the lepton transverse momentum spectra because it is to first order independent of the transverse momentum of the W . Under transverse Lorentz boosts along a direction ϕ^* , M_T and $p_T(e)$ transform as

$$M_T^2 \cong M_T^{*2} - \beta^2 \cos^2 \phi^* M_L^{*2},$$

$$p_T(e) \cong p_T^*(e) + \frac{1}{2} p_T(W) \cos \phi^*,$$

with $M_T^* = M_W \sin \theta^*$, $M_L^* = M_W \cos \theta^*$ and $\beta = p_T(W)/M_W$. The asterisk indicates quantities in the W rest frame. The disadvantage of using the transverse mass is that it uses the neutrino transverse momentum which is a derived quantity. The neutrino transverse momentum is identified with the missing transverse energy in the event, which is given by

$$\vec{E}_T = - \sum_i \vec{p}_{T_i} = -\vec{p}_T(e) - \vec{p}_T^{rec} - \vec{u}_T(\mathcal{L}),$$

where \vec{p}_T^{rec} is the transverse momentum of the W -recoil system and $\vec{u}_T(\mathcal{L})$ the transverse energy flow of the underlying event, which depends on the luminosity. It then follows that the magnitude of the missing E_T vector and the true neutrino momentum are related as

$$E_T = p_T(\nu) + \frac{1}{4} \frac{u_T^2}{p_T(\nu)}. \quad (40)$$

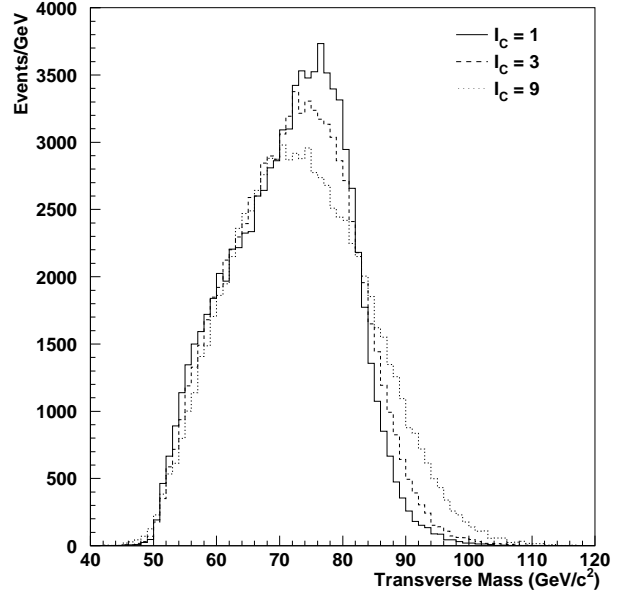


Figure 13: The effect of multiple interactions on the W transverse mass distribution at the Tevatron. Standard kinematic cuts of $p_T(e) > 25$ GeV/c, $|\eta(e)| < 1.2$, $\vec{E}_T > 25$ GeV and $p_T(W) < 30$ GeV/c are imposed. The effect of multiple interactions is simulated by adding additional minimum bias events to the event containing the W boson.

This relation can be interpreted as the definition of the neutrino momentum scale. Note that the underlying event gives rise to a bias in the *measured* neutrino momentum with respect to the *true* neutrino momentum. In case there are more interactions per crossing, $|\vec{u}_T|$ behaves as a two-dimensional random walk and is proportional to $\sqrt{I_C}$, where I_C is the average number of interactions per crossing. The shift in measured neutrino momentum is thus directly proportional to the number of interactions per crossing. The resolution increases as $\sqrt{I_C}$.

The above equation for the missing transverse energy deserves some more attention. The two components directly related to the W decay, $\vec{p}_T(e)$ and \vec{p}_T^{rec} , are only indirectly affected by multiple interactions through the underlying event. It is the measurement of $\vec{u}_T(\mathcal{L})$ which governs the luminosity dependence. Because of multiple interactions, $\vec{u}_T(\mathcal{L})$ will show a dependence on luminosity following Poisson statistics, with the two effects indicated above: *i*) a degradation of the E_T resolution and *ii*) a shift in the measured neutrino momentum. This is demonstrated in Fig. 13 where we show the M_T distribution for various values of I_C at the Tevatron. For Run II one expects $I_C \approx 3$, and at TeV33, $I_C \approx 6 - 9$ [37]. Both effects, of course, propagate into the measurement of the transverse mass and the uncertainty on M_W will not follow the simple $1/\sqrt{N}$ rule anymore [38]. In addition, however, the detector response to high luminosities needs to be folded in. In the

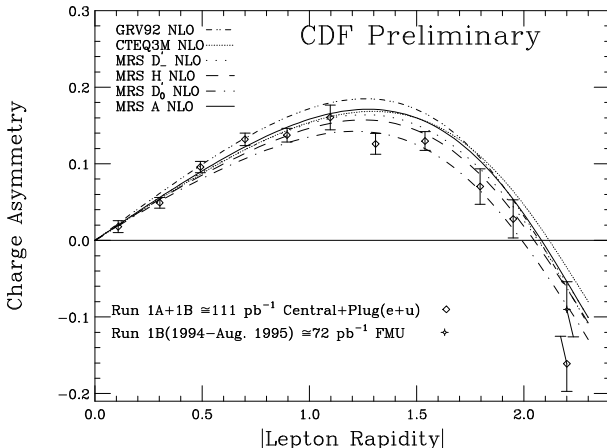


Figure 14: Comparison of the CDF W asymmetry measurement with recent NLO parton distribution function predictions.

above discussion it was assumed that the detector response is linear to the number of multiple interactions which in general is not the case. The effects of pile-up in the calorimeter and occupancy in the tracking detectors produce a $\sim 7\%$ shift in p_T for an electron with transverse momentum of 40 GeV/c at $\mathcal{L} = 10^{33} \text{ cm}^{-2} \text{ s}^{-1}$, which will further affect the uncertainty on the W mass adversely [39].

Another uncertainty that will not, and has not in the past, scaled with luminosity is the theoretical uncertainty coming from the $p_T(W)$ model and the uncertainty on the proton structure. Parton distributions and the spectrum in $p_T(W)$ are correlated. The DØ experiment has addressed this correlation in the determination of its uncertainty on the W mass [4, 5]. The parton distribution functions are constrained by varying the CDF measured W charge asymmetry within the measurement errors, while at the same time utilizing all the available data. New parametrizations of the CTEQ 3M parton distribution function were obtained that included in the fit the CDF W asymmetry data from Run Ia [40], where all data points had been moved coherently up or down by one standard deviation. In addition one of the parameters, which describes the Q^2 -dependence of the parameterization of the non-perturbative functions describing the $p_T(W)$ spectrum [41], was varied. The constraint on this parameter was provided by the measurement of the $p_T(Z)$ spectrum. The uncertainty due to parton distribution functions and the $p_T(W)$ input spectrum was then assessed by varying simultaneously the parton distribution function, as determined by varying the measured W charge asymmetry, and the parameter describing the non-perturbative part of the $p_T(W)$ spectrum.

The CDF experiment uses their measurement of the W charge asymmetry as the sole constraint on the uncertainty due to the parton distribution functions. Figure 14 compares the preliminary CDF W charge asymmetry measurement [42] with several recent fits to parton distribution functions. Figure 15 shows the

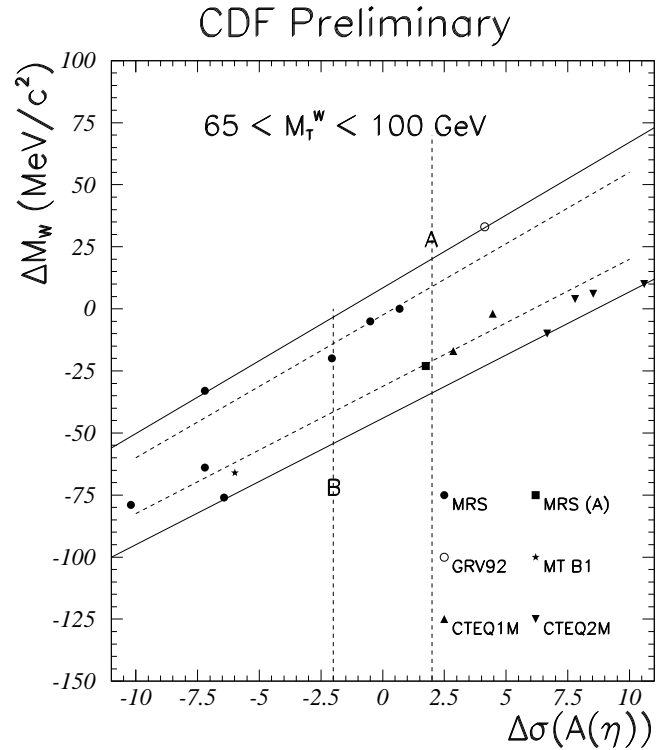


Figure 15: The correlation between the uncertainty in the W mass and the deviation between the average measured asymmetry for Run Ia and Ib CDF data for several recent parton distribution functions .

correlation between the uncertainty on the W mass, ΔM_W , and

$$\Delta\sigma(A(\eta)) = \frac{\langle A_{PDF}(\eta) \rangle - \langle A_{data}(\eta) \rangle}{\delta A_{data}(\eta)}, \quad (41)$$

the deviation between the average measured asymmetry for Run Ia and Ib data and various recent NLO parton distribution function fits [42]. The fitted W mass is seen to be strongly correlated with the W charge asymmetry. The W charge asymmetry, however, is mainly sensitive to the slope of the ratio of the u and d quark parton distribution functions

$$A(y_W) \propto \frac{d(x_2)/u(x_2) - d(x_1)/u(x_1)}{d(x_2)/u(x_2) + d(x_1)/u(x_1)} \quad (42)$$

and does not probe the full parameter range describing the parton distribution functions .

Future measurements of the $p_T(Z)$ distribution will provide a constraint on the p_T distribution of the W boson. Moreover, the measurements of the W charge asymmetry, together with measurements from deep inelastic scattering experiments, will provide further constraints on the parton distribution functions. An effort needs to be made, though, to provide the experiments with parton distributions with associated uncertainties.

At high luminosities alternate methods to determine the W -mass may be advantageous. Because of the similarity of W and

Z production, methods based on ratios of relevant quantities, such as the charged lepton transverse momenta are particularly interesting [43, 44]. The ratio of the lepton p_T distributions is thought to be very promising for fitting the W mass in the high luminosity regime since the procedure is independent of many resolution effects. However, the shapes of the lepton transverse momentum distributions are sensitive to the differences in the W and Z production mechanisms, which need to be better understood.

Here we concentrate on a similar method which utilizes the transverse mass ratio of W and Z bosons [44]. Preliminary results from an analysis of the transverse mass ratio have recently been presented by the DØ Collaboration [45]. Only the electron channel will be discussed in the following, although the method is expected to work for muon final states as well.

The transverse mass ratio method treats the $Z \rightarrow e^+e^-$ sample similar to the $W \rightarrow e\nu$ sample, thus cancelling many of the common systematic uncertainties. A transverse mass for the Z boson is constructed with one of the decay electrons, while the E_T is derived by adding the transverse energy of the other electron to the residual E_T in the event. Hence, two such combinations can be formed for each Z event.

The Z transverse mass distribution is scaled down in finite steps and compared with the M_T distribution of the W boson. The W mass is then determined from the scale factor (M_W/M_Z) which gives the best agreement between the M_T distributions using a Kolmogorov test. Since differences in the production mechanism, acceptances and resolution effects between the W and the Z sample lead to differences in the shapes of the transverse mass distributions, one has to correct for these effects.

The dominant systematic uncertainty arises from the uncertainty on the underlying event. Electromagnetic and hadronic resolution effects mostly cancel in the transverse mass ratio, as expected. The systematic uncertainty due to the parton distribution functions and the transverse momentum of the W boson is reduced by more than a factor 3 compared with that found using the conventional W transverse mass method [4]. The total systematic error from the DØ Run Ia data sample is estimated to be 75 MeV/c 2 . For comparison, the total systematic error obtained using the transverse mass distribution of the W using DØ Run Ia data is 165 MeV/c 2 [4].

In the analysis of the Run Ia data sample, electrons from W and Z decay are identified as in the conventional W mass analysis. W candidates are selected by requiring $p_T(e) > 30$ GeV/c and $p_T(\nu) > 30$ GeV/c, while electrons from Z decays are required to have $p_T(e) > 34$ GeV/c, since they are eventually scaled down. Electrons from W decay and at least one electron from Z decay are required to be in the central pseudorapidity region, $|\eta(e)| < 1.1$. Z events are used twice if both electrons fall in the central region. The shape comparison is performed in the fitting window 65 GeV/c $^2 < M_T < 100$ GeV/c 2 . The selected Z sample is scaled down in finite steps and, at every step, the shape of the Z and W M_T distribution is compared using the Kolmogorov test. Figure 16 shows the $M_T(Z)$ distribution superimposed on the $M_T(W)$ distribution for one of the fits. The preliminary result for M_W from Run Ia data is

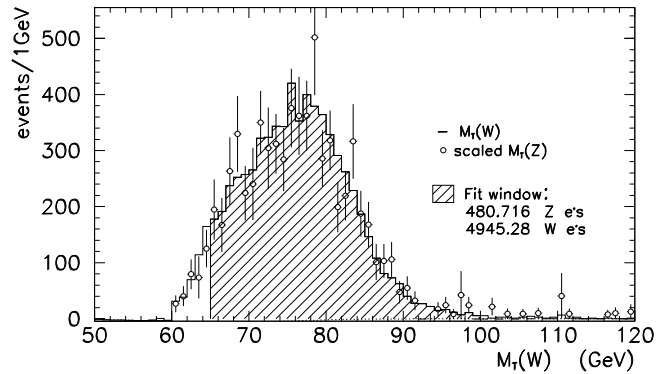


Figure 16: The Run Ia DØ $M_T(W)$ distribution (histogram) with the scaled $M_T(Z)$ distribution (points) superimposed.

$$M_W = 80.160 \pm 0.360(\text{stat}) \pm 0.075(\text{syst}) \text{ GeV}/c^2. \quad (43)$$

The limitation of the method described here comes entirely from the limited Z statistics, which is expected to scale exactly as $1/\sqrt{N}$ in future experiments.

The power of the M_T ratio method becomes apparent when one compares the uncertainty on M_W expected for 1 fb^{-1} and 10 fb^{-1} with that expected from the traditional W transverse mass analysis [38]. The results for both methods are listed in Table II. To calculate the projected statistical (systematic) errors in the transverse mass ratio method, we have taken the errors of Eq. (43) and scaled them with $1/\sqrt{N}$ ($\sqrt{I_C/N}$), assuming $I_C = 3$ ($I_C = 9$) for 1 fb^{-1} (10 fb^{-1}). Both, electron and muon channels are combined in Table II, assuming that the two channels yield the same precision in M_W .

Table II: Projected statistical and systematic errors (per experiment) on the W mass at the Tevatron, combining the $W \rightarrow e\nu$ and $W \rightarrow \mu\nu$ channel.

traditional M_T analysis		
δM_W	$\int \mathcal{L} dt = 1 \text{ fb}^{-1}$	$\int \mathcal{L} dt = 10 \text{ fb}^{-1}$
statistical	$I_C = 3$	$I_C = 9$
systematic	29 MeV/c 2	17 MeV/c 2
total	42 MeV/c 2	23 MeV/c 2
	51 MeV/c 2	29 MeV/c 2

W/Z transverse mass ratio		
δM_W	$\int \mathcal{L} dt = 1 \text{ fb}^{-1}$	$\int \mathcal{L} dt = 10 \text{ fb}^{-1}$
statistical	$I_C = 3$	$I_C = 9$
systematic	29 MeV/c 2	9 MeV/c 2
total	10 MeV/c 2	6 MeV/c 2
	31 MeV/c 2	11 MeV/c 2

The W mass can also be determined from the transverse energy (momentum) distribution of the electron (muon) in $W \rightarrow$

$e\nu_e$ ($W \rightarrow \mu\nu_\mu$) events, which peaks at $M_W/2$. The prospects of a precise measurement of M_W from the $E_T(e)$ distribution in Run II and at TeV33 have been investigated in Ref. [39]. The measurement of the lepton four-momentum vector is independent of the E_T resolution, and the electron E_T resolution is dominated by the intrinsic calorimeter resolution. Hence the statistical uncertainty of the W mass measurement from the $E_T(e)$ distribution is expected to scale approximately as $1/\sqrt{N}$. Simulations have shown that a sample of 30,000 events (similar to the DØ Run Ib data sample) gives a statistical error on the W mass of 100 MeV/c 2 from the $E_T(e)$ fit. This is in agreement with the result of the preliminary DØ Run Ib W mass analysis [46]. The systematic error from this method is expected to be about 170 MeV/c 2 for the same number of events. Scaling the total uncertainty as $1/\sqrt{N}$, the projected uncertainty of M_W from the electron E_T fit is:

$$\begin{aligned}\delta M_W &= 55 \text{ MeV/c}^2 \quad \text{for } 1 \text{ fb}^{-1}, \\ \delta M_W &= 18 \text{ MeV/c}^2 \quad \text{for } 10 \text{ fb}^{-1}.\end{aligned}\quad (44)$$

In estimating the uncertainties given in Eq. (44) and Table II, we have assumed that the current uncertainty from parton distribution functions and the theoretical uncertainty originating from higher order electroweak corrections can be drastically reduced in the future. In order to measure M_W with high precision, it is crucial to fully control higher order electroweak (EW) corrections. So far, only the final state $\mathcal{O}(\alpha)$ photonic corrections have been calculated [47], using an approximation which indirectly estimates the soft + virtual part from the inclusive $\mathcal{O}(\alpha^2)$ $W \rightarrow \ell\nu(\gamma)$ width and the hard photon bremsstrahlung contribution. Using this approximation, electroweak corrections were found to shift the W mass by about -65 MeV/c 2 in the electron, and -170 MeV/c 2 in the muon channel [4, 5].

Currently, a more complete calculation of the $\mathcal{O}(\alpha)$ EW corrections, which takes into account initial and final state corrections, is being carried out [48]. The calculation is performed using standard Monte Carlo phase space slicing techniques for NLO calculations. In calculating the initial state radiative corrections, mass (collinear) singularities are absorbed into the parton distribution functions through factorization, in complete analogy to the QCD case. QED corrections to the evolution of the parton distribution function are not taken into account. A study of the effect of QED on the evolution indicates that the change in the scale dependence of the PDF is small [49]. To treat the QED radiative corrections in a consistent way, they should be incorporated in the global fitting of the PDF. The relative size and the characteristics of the various contributions to the EW corrections to W production is shown in Fig. 17.

Initial state (photon and weak) radiative corrections are found to be uniform and, therefore, are expected to have little effect on the W boson mass extracted. While initial state photon radiation increases the cross section by 0.9%, weak one-loop corrections almost completely cancel the initial state photonic corrections. The complete $\mathcal{O}(\alpha)$ initial state EW corrections reduce the leading order (LO) cross section by about 0.1%. Initial and final state photon radiation interfere very little. The interference effects are uniform and have essentially no effect on the M_T distribution. Final state photon radiation changes the shape of the

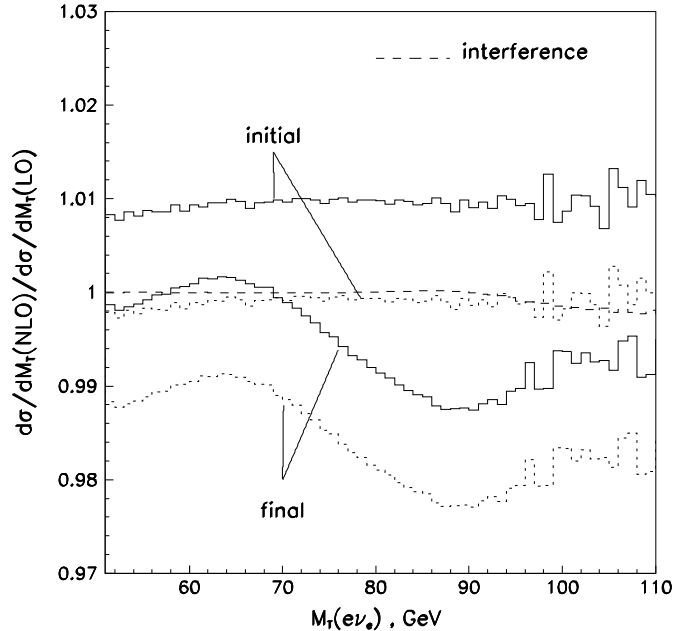


Figure 17: The ratio of the NLO to LO $M_T(e\nu_e)$ distribution for various individual contributions: the QED-like initial or final state contributions (solid), the complete $\mathcal{O}(\alpha)$ initial and final state contributions (short dashed) and the initial–final state interference contribution (long dashed).

transverse mass distribution and reduces the LO cross section by up to 1.4% in the W resonance region. Weak corrections again have no influence on the lineshape, but reduce the cross section by about 1%. The W mass obtained from the M_T distribution including the full EW one-loop corrections is expected to be several MeV/c 2 smaller than that extracted employing the approximate calculation of Ref. [47].

Since final state photon radiation introduces a significant shift in the W mass, one also has to worry about multiple photon radiation. A calculation of $p\bar{p} \rightarrow \mu\nu\gamma\gamma$ [50] which includes all initial and final state radiation and finite muon mass effects shows that approximately 0.8% of all $W \rightarrow \mu\nu$ events contain two photons with $E_T(\gamma) > 0.1$ GeV (the approximate tower threshold of the electromagnetic calorimeters of CDF and DØ) and $\Delta R(\gamma, \gamma) > 0.14$. This suggests that the additional shift in M_W from multiple photon radiation may not be negligible if one aims at a measurement with a precision of $\mathcal{O}(10 \text{ MeV/c}^2)$.

4. LHC

At the LHC, the cross section for W production is about a factor 4 larger than at the Tevatron. During the first year of operation, it is likely that the LHC will run at a reduced luminosity of approximately $\mathcal{L} = 10^{33} \text{ cm}^{-2} \text{ s}^{-1}$, resulting in roughly 0.9×10^7 $W \rightarrow e\nu$ events with a central electron ($|\eta(e)| < 1.2$) and a transverse mass in the range $65 \text{ GeV/c}^2 < M_T < 100 \text{ GeV/c}^2$. A similar number of $W \rightarrow \mu\nu$ events

is expected. Both LHC detectors, ATLAS [24] and CMS [25], will be able to trigger on electrons and muons with a transverse momentum of $p_T(\ell) > 15 \text{ GeV}/c$ ($\ell = e, \mu$), and should be fully efficient for $p_T(\ell) > 20 \text{ GeV}/c$. They are well-optimized for electron, muon and E_T detection.

At $\mathcal{L} = 10^{33} \text{ cm}^{-2} \text{ s}^{-1}$, the average number of interactions per crossing at the LHC is approximately $I_C = 2$, which is significantly smaller than what one expects at the Tevatron for the same luminosity. A precision measurement of the W mass at the LHC running at a reduced luminosity, using the traditional transverse mass analysis, thus seems feasible [51].

QCD corrections to the transverse mass distribution at the LHC enhance the cross section by 10 – 20% in the M_T range which is normally used to determine M_W . This is illustrated in Fig. 18, where the LO and NLO QCD transverse mass distribution is shown, together with the NLO to LO differential cross section ratio. Here, a $p_T(\ell) > 20 \text{ GeV}/c$ and a $\not{p}_T > 20 \text{ GeV}/c$ cut have been imposed, and the pseudorapidity of the lepton is required to be $|\eta(\ell)| < 1.2$. The slight change in the shape of the M_T distribution induced by the NLO QCD corrections is due to the cuts imposed.

So far, no detailed study of the precision which one might hope to achieve for M_W at the LHC has been performed. For a *crude order of magnitude* estimate, one can use the statistical and systematic errors of the current CDF and DØ analyses [4, 5], and scale them by $\sqrt{I_C/N}$. For an integrated luminosity of 10 fb^{-1} , one obtains [51]:

$$\delta M_W \lesssim 15 \text{ MeV}/c^2. \quad (45)$$

In order to see whether LHC experiments can perform a measurement of M_W which is significantly more precise than what one expects from TeV33 or the NLC, a more detailed study which also considers other quantities such as the transverse mass ratio of W and Z bosons [43, 44] has to be carried out.

5. Constraints on M_H from M_W and M_t

The potential of extracting useful information on the Higgs boson mass from a fit to the SM radiative corrections and a precise measurement of M_W and M_t is illustrated in Fig. 19. Here we have assumed $M_t = 176 \pm 2 \text{ GeV}/c^2$, $M_W = 80.330 \pm 0.010 \text{ GeV}/c^2$, and $\alpha^{-1}(M_Z^2) = 128.89 \pm 0.05$. Such a measurement would constrain the Higgs boson mass to $M_H = 285^{+65}_{-55} \text{ GeV}/c^2$. The corresponding log-likelihood function is shown in Fig. 20. A measurement of the W mass with a precision of $\delta M_W = 10 \text{ MeV}/c^2$ and of the top mass with an accuracy of $2 \text{ GeV}/c^2$ thus translates into an indirect determination of the Higgs boson mass with a relative error of about

$$\delta M_H/M_H \approx 20\%. \quad (46)$$

From a global analysis of all electroweak precision data one might then expect $\delta M_H/M_H < 15\%$.

For the precision of M_t and M_W assumed here, the theoretical error from higher orders and the uncertainty in the electromagnetic coupling constant $\alpha(M_Z^2)$ become limiting factors for the accuracy which can be achieved for M_H . Efforts to calculate higher order corrections and to significantly improve the error

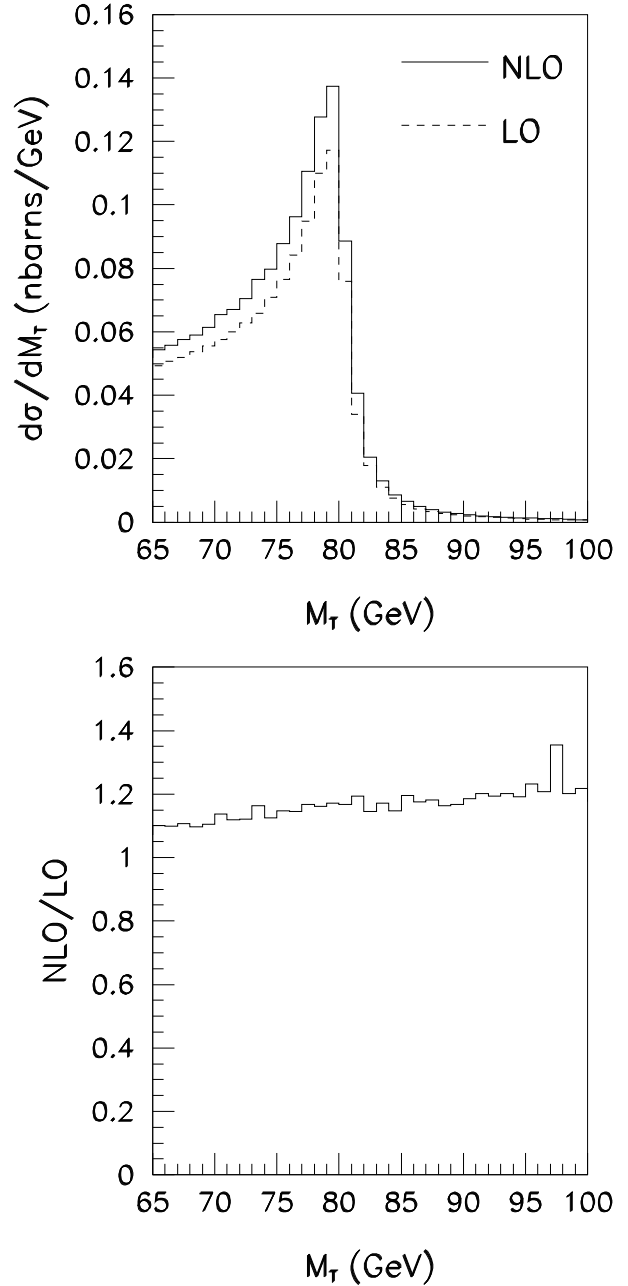


Figure 18: The LO and NLO QCD W transverse mass distribution at the LHC. Also shown is the NLO to LO differential cross section ratio as a function of M_T .

on $\alpha(M_Z^2)$ beyond what one can expect from measurements at Novosibirsk, DAPΦNE, or BES, need increased emphasis from both experimentalists and theorists in order to be able to achieve an ultimate relative precision on M_H better than about 15%.

M_W vs. M_H

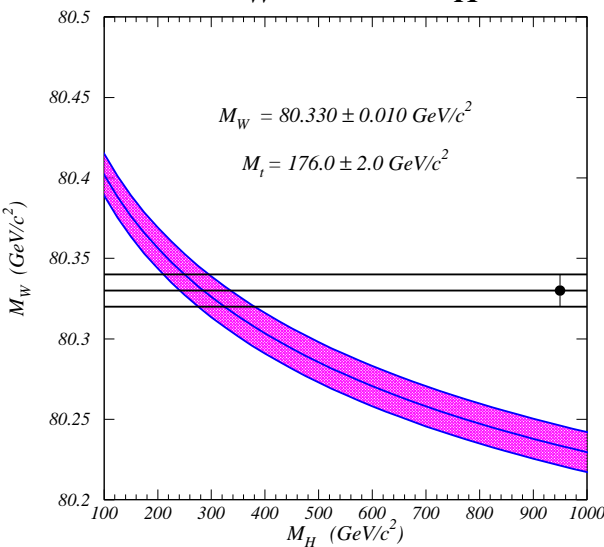


Figure 19: Predicted W versus Higgs boson mass for $M_t = 176 \pm 2 \text{ GeV}/c^2$. The theoretical predictions incorporate the effects of higher order electroweak and QCD corrections.

$-\text{Log}(L)$ vs. M_H

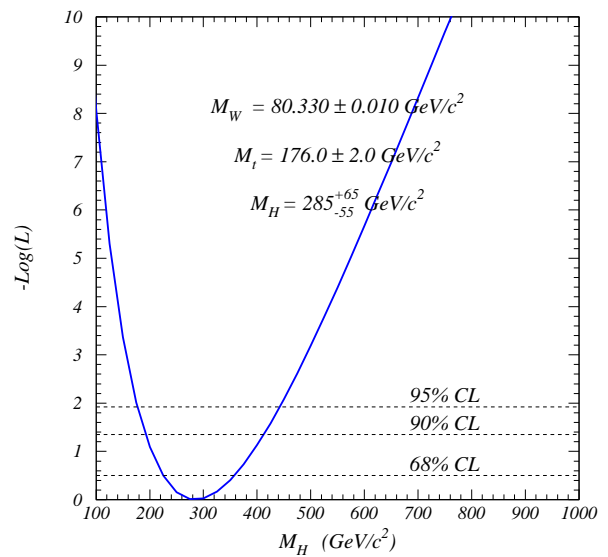


Figure 20: The negative log-likelihood function assuming $M_W = 80.330 \pm 0.010 \text{ GeV}/c^2$ and $M_t = 176 \pm 2 \text{ GeV}/c^2$.

IV. SUMMARY AND CONCLUSIONS

In this report, we have highlighted some current high precision electroweak measurements, and explored prospects for further improvements over the next decade. The aim of precision electroweak measurements is to test the SM at the quantum level, and to extract indirect information on the mass of the Higgs boson. The confrontation of these indirect predictions of M_H with the results of direct searches for the Higgs boson will be perhaps the most exciting development of the next decade in the field of particle physics.

Although a global fit to all available precision electroweak data yields $M_H = 149^{+148}_{-82} \text{ GeV}/c^2$, the Higgs boson mass extracted strongly depends on the input quantities used in the fit. Excluding a particular observable which displays a statistically significant deviation from the SM prediction, e.g. the SLD left-right asymmetry, may easily increase the central value of M_H by a factor 4. One therefore has to conclude that present data are not quite sufficient to obtain a stable estimate of the Higgs boson mass.

Results of future collider experiments are expected to drastically change this situation. In these experiments one hopes to precisely determine three observables which are key ingredients in obtaining reliable indirect information on the Higgs boson mass:

- The uncertainty on the top quark mass is expected to be reduced by at least a factor 3 in Tevatron and LHC experiments. At the NLC or a $\mu^+ \mu^-$ collider, a precision of a

few hundred MeV/c^2 may be possible.

- It should be possible to reduce the error on $\sin^2 \theta_{\text{eff}}^{\text{lept}}$ by at least a factor two through measurements of the left-right asymmetry at a luminosity upgraded SLC, and the forward backward asymmetry in the Z peak region at the Tevatron and LHC.
- The most profound improvement is likely to occur for the W mass, where a gain of a factor 5 seems to be within reach. New strategies developed for extracting M_W at hadron colliders [43, 44] will make it possible to fully exploit the expected increase in integrated luminosity at the Tevatron.

From a measurement of M_t with a precision of $2 \text{ GeV}/c^2$, and M_W with an uncertainty of $10 \text{ MeV}/c^2$ alone it should be possible to constrain M_H within 20%.

As the electroweak measurements improve, the theoretical error from higher orders and the uncertainty in $\alpha(M_Z^2)$ will gradually become more and more important limitations in the precision which can be achieved. The determination of $\alpha(M_Z^2)$ is limited by the knowledge of the photon hadron coupling at small momentum transfer. An increased experimental and theoretical effort is needed to overcome the present limitations in determining $\alpha(M_Z^2)$, and to calculate higher order corrections to the electroweak observables.

V. REFERENCES

- [1] *M. Demarteau*, FERMILAB-Conf-96/354, to appear in the Proceedings of the *DPF96 Conference*, Minneapolis, MN, August 10 – 15, 1996.
- [2] *R.M. Barnett et al. (Particle Data Group)*, Phys. Rev. **D54**, 1 (1996).
- [3] *D. Gerdes*, these proceedings.
- [4] *F. Abe et al. (CDF Collaboration)*, Phys. Rev. Lett. **75**, 11 (1995) and Phys. Rev. **D52**, 4784 (1995); *S. Abachi et al. (DØ Collaboration)* Phys. Rev. Lett. **77**, 3309 (1996).
- [5] *S. Abachi et al. (DØ Collaboration)* FERMILAB-Conf/96-251-E, submitted to the “*28th International Conference on High Energy Physics*”, Warsaw, Poland, 25 – 31 July 1996.
- [6] *H. Burkhardt and B. Pietrzyk*, Phys. Lett. **B356**, 398 (1995); *S. Eidelmann and F. Jegerlehner*, Z. Phys. **C67**, 585 (1995); *R.B. Nezvorov, A.V. Novikov and M.I. Vysotsky*, JETP Lett. **60**, 399 (1994); *A.D. Martin and D. Zeppenfeld*, Phys. Lett. **B345**, 558 (1995); *M. Swartz*, Phys. Rev. **D53**, 5268 (1996).
- [7] *N. Cabibbo and R. Gatto*, Phys. Rev. **124**, 1577 (1961).
- [8] *P. Gambino and A. Sirlin*, Phys. Rev. **D49**, 1160 (1994).
- [9] *G. Altarelli*, CERN-TH/96-265 (November 1996), lectures given at the NATO Advanced Study Institute on Techniques and Concepts of High Energy Physics, St. Croix, U.S. Virgin Islands, 10 – 23 July, 1996.
- [10] *J. Rosner*, CERN-TH/96-245, hep-ph/9610222, lectures given at the Cargèse Summer Institute on Particle Physics, 1996.
- [11] *P. Chankowski et al.*, Nucl. Phys. **B417**, 101 (1994); *A. Dabelstein et al.*, in Proceedings of the “*Ringberg Workshop on Perspectives for Electroweak Interactions in e^+e^- Collisions*”, Ringberg, Germany, February 5 – 8, 1995; *D. Pierce et al.*, SLAC-PUB-7180, preprint, June 1996.
- [12] *D. Gerdes et al.*, these proceedings.
- [13] *D. Amidei et al.*, in “*Future Electroweak Physics at the Fermilab Tevatron: Report of the tev_2000 Study Group*”, eds. D Amidei and R. Brock, FERMILAB-Pub/96-082 (1996), p. 13.
- [14] *S. Kuhlmann et al.*, “*Physics and Technology of the Next Linear Collider*”, FERMILAB Pub-96/112 (1996).
- [15] *R. Palmer et al.*, “ $\mu^+\mu^-$ Collider: A Feasibility Study”, FERMILAB-Conf-96/092 (1996).
- [16] *M. Breidenbach et al.*, SLAC-CN-409 (1996).
- [17] *K. Abe et al. (SLD Collaboration)*, Phys. Rev. Lett. **74**, 2890 (1995).
- [18] *J. Collins and D. Soper*, Phys. Rev. **D16**, 2219 (1977).
- [19] *C. Albajar et al. (UA1 Collaboration)*, Z. Phys. **C44**, 15 (1989); *F. Abe et al. (CDF Collaboration)*, Phys. Rev. Lett. **67**, 1502 (1991).
- [20] *F. Abe et al. (CDF Collaboration)*, Phys. Rev. Lett. **77**, 2616 (1996).
- [21] *U. Baur, S. Keller and W. Sakumoto*, in preparation.
- [22] *P. Fisher, U. Becker and P. Kirkby*, Phys. Lett. **B356**, 404 (1995).
- [23] *M. Dittmar*, ETHZ-IPP PR-96-01 (preprint, March 1996), to appear in Phys. Rev. **D**.
- [24] *D. Gingrich et al. (ATLAS Collaboration)*, ATLAS Letter of Intent, CERN-LHCC-92-4 (October 1992); *W. W. Armstrong et al. (ATLAS Collaboration)*, ATLAS Technical Design Report, CERN-LHCC-94-43 (December 1994).
- [25] *M. Della Negra et al. (CMS Collaboration)*, CMS Letter of Intent, CERN-LHCC-92-3 (October 1992); *G. L. Bayatian et al. (CMS Collaboration)*, CMS Technical Design Report, CERN-LHCC-94-38 (December 1994).
- [26] *K. Kumar*, these proceedings.
- [27] *F. Cuypers and P. Gambino*, Phys. Lett. **B388**, 211 (1996).
- [28] *W.J. Marciano and A. Sirlin*, Phys. Rev. **D22**, 2695 (1980); *R.G. Stuart*, Z. Phys. **C34**, 445 (1987).
- [29] *K.S. McFarland et al. (CCFR/NuTeV Collaboration)*, FERMILAB-Conf-96/227-E, to appear in the Proceedings of the “*XXXIst Rencontres de Moriond, Electroweak Interactions and Unified Theories*”, Les Arcs, France, March 16 – 23, 1996.
- [30] *J. Allaby et al. (CHARM Collaboration)*, Z. Phys. **C36**, 611 (1985); *A. Blondel et al. (CDHS Collaboration)*, Z. Phys. **C45**, 361 (1990); *C. Arroyo et al. (CCFR Collaboration)*, Phys. Rev. Lett. **72**, 3452 (1994).
- [31] *R.J. Cashmore et al.*, MPI/PTh/96-105, to appear in the “*Proceedings of the Workshop on Future Physics at HERA*”.
- [32] *A. Ballestrero et al.*, in Proceedings of the Workshop on Physics at LEP2, G. Altarelli, T. Sjostrand and F. Zwirner (eds.), CERN Yellow Report CERN-96-01 (1996), Vol. 1, p. 141.
- [33] *W.J. Stirling*, Nucl. Phys. **B456**, 3 (1995).
- [34] *K. Ackerstaff et al. (OPAL Collaboration)*, CERN-PPE/96-141 (preprint, October 1996), submitted to Phys. Lett. **B**; *N. Watson (OPAL Collaboration)*, talk given at CERN, October 1996; *M. Pohl (L3 Collaboration)*, talk given at CERN, October 1996.
- [35] *T. Sjöstrand and V. Khoze*, Z. Phys. **C62**, 281 (1994); Phys. Rev. Lett. **72**, 28 (1994).
- [36] *L. Lönnblad and T. Sjöstrand*, Phys. Lett. **B351**, 293 (1995).
- [37] *G. Jackson*, these proceedings; *M. Johnson*, these proceedings.
- [38] *U. Baur, M. Demarteau, and S. Errede*, in “*Future Electroweak Physics at the Fermilab Tevatron: Report of the tev_2000 Study Group*”, eds. D Amidei and R. Brock, FERMILAB-Pub/96-082 (1996), p. 63.
- [39] *A.V. Kotwal*, these proceedings.
- [40] *F. Abe et al. (CDF Collaboration)*, Phys. Rev. Lett. **74**, 850 (1995).
- [41] *G. Ladinsky and C.-P. Yuan*, Phys. Rev. **D50**, 4239 (1994).
- [42] *A. Bodek (CDF Collaboration)*, FERMILAB-Conf/96-341-E preprint, to appear in the Proceedings of the “*28th International Conference on High Energy Physics*”, Warsaw, Poland, 25 – 31 July 1996.
- [43] *W. Giele and S. Keller*, FERMILAB-Conf-96/307-T, to appear in the Proceedings of the *DPF96 Conference*, Minneapolis, MN, August 10 – 15, 1996.
- [44] *S. Rajagopalan and M. Rijssenbeek*, these proceedings.
- [45] *M. L. Kelly et al. (DØ Collaboration)*, FERMILAB-Conf/96-236-E, to appear in the Proceedings of the *DPF96 Conference*, Minneapolis, MN, August 10 – 15, 1996.
- [46] *M. Rijssenbeek*, FERMILAB-Conf/96-365-E, to appear in the Proceedings of the “*28th International Conference on High Energy Physics*”, Warsaw, Poland, 25 – 31 July 1996.

- [47] *F. Berends and R.K. Kleiss*, Z. Phys. **C27**, 365 (1985).
- [48] *U. Baur, S. Keller and D. Wackerlo*, these proceedings and paper in preparation.
- [49] *H. Spiesberger*, Phys. Rev. **D52**, 4936 (1995); *J. Kripfganz and H. Perlt*, Z. Phys. **C41**, 319 (1988).
- [50] *U. Baur, T. Han, R. Sobey and D. Zeppenfeld*, these proceedings.
- [51] *S. Keller and J. Womersley*, these proceedings.